Available online at www.sciencedirect.com
SCIENCE DIRECT®
Journal of Molecular Catalysis A: Chemical 223 (2004) 275–281
JOURNAL OF MOLECULAR CATALYSIS A: CHEMICAL
www.elsevier.com/locate/molcata

Role of substitution in catalytic activity of La–Th–V–O mixed oxides for the reaction of methanol

Mrinal R. Pai, B.N. Wani, A.D. Belapurkar, N.M. Gupta*

Applied Chemistry Division, Bhabha Atomic Research Centre, Trombay, Mumbai 400085, India

Received 15 February 2003; received in revised form 24 August 2003; accepted 1 September 2003
Available online 16 September 2004

Abstract

A series of composite metal oxide catalysts of nominal composition $La_xTh_{1-x}V_2O_{7-\delta}$ ($x = 0.0$–0.5) were synthesized by ceramic route and characterized using XRD, IR and temperature programmed reduction (TPR) measurements. The partial substitution at A-sites had profound effect on the catalytic behavior of thorium pyrovanadate for the dehydration of methanol, the extent of which depended upon the value of x. The following was the trend of catalytic activity of different samples as a function of the value of x: x up to $0.2 > 0.3 > 0.5 > 0 > ThO_2$. In addition, the substituted samples exhibited higher selectivity for the formation of dimethyl ether and also a better compositional stability towards the successive cycles of reduction/reoxidation. These characteristics of substituted samples are found to be related to existence of a phase, viz. $La_xTh_{1-x}V_2O_{7-\delta}$, where a part of lattice Th sites are substituted by La. On the other hand, the other secondary phases, viz. $LaTh(VO_4)_{3-\delta}$ and $Th(VO_3)_4$ that were produced simultaneously during the sample preparation, play no important role. It is suggested that the nonstoichiometry generated in the pyrovanadate phase is responsible to the improvement in the catalytic activity and the stability of the substituted samples.

Keywords: Catalytic activity; Nonstoichiometry; Dimethyl ether; Thorium vanadate

1. Introduction

The oxides of vanadium serve as efficient catalysts for the selective oxidation and oxidative dehydrogenation of hydrocarbons, depending upon the valence state of vanadium and the surface characteristics [1]. The catalytic behavior is also found to be different for the multi-component metal oxides containing vanadium and also when one or more of the metal sites are substituted partially with other aliovalent metal ions. The identification of the physico-chemical changes arising due to such substitutions and to pin point the resulting crystallographic phases which eventually modify the catalytic behavior are however some of the areas that still require in-depth investigations. With these considerations in mind we have investigated the redox properties, thermal behavior and the catalytic activity of B-site substituted thorium metavanadates, i.e. $Th(Mn_xV_{1-x}O_{3-\delta})_4$ and reported recently that the samples with $x = 0.2$ exhibited higher catalytic activity for oxidation of carbon monoxide in addition to improved phase stability. These changes have been attributed to nonstoichiometry generated as a result of substitution [2,3]. In continuation to these previous studies, we have now investigated the catalytic activity of thorium pyrovanadate (ThV_2O_7), in view of its thermally stable pyrochlore structure. The substitution at A-site by La was aimed at generating nonstoichiometry in the lattice so as to improve the catalytic activity. With this in view, different ThV_2O_7 samples with substitution of up to 50% of Th by La were synthesized and were characterized using XRD, and IR spectroscopy measurements. The repeated cycles of temperature programmed reduction (TPR) followed by temperature programmed oxidation (TPO) were recorded in order to study the phase stability

* Corresponding author. Tel.: +91 22 25505146; fax: +91 22 25505151/25519613.
E-mail address: nmgupta@magnum.barc.ernet.in (N.M. Gupta).

1381-1169/$ – see front matter © 2004 Elsevier B.V. All rights reserved.
doi:10.1016/j.molcata.2003.09.045

of these oxides during the process of reduction/reoxidation. The catalytic activity of these samples was evaluated for the reaction of methanol at different temperatures.

2. Experimental

2.1. Catalyst preparation

Mixed oxides $La_xTh_{1-x}V_2O_{7-\delta}$ with nominal composition (x = 0.0–0.5) were synthesized by ceramic route as per the following equation:

$$2(1-x)ThO_2 + xLa_2O_3 + 2V_2O_5 \rightarrow 2La_xTh_{1-x}V_2O_{7-\delta}$$

The sample pellets were calcined in two steps in order to prevent the melting of V_2O_5 (m.p. 690 °C). The first heating was done at 600 °C for 2 days followed by prolonged heating at 750 °C for 3 days with two intermittent grindings so as to ensure the phase uniformity and the completion of reaction. The final samples were found to be stable when heated in air up to 900 °C. For the sake of brevity, the mixed oxide samples are referred in the text as La(20), La(30), etc., where the figures in parentheses represent the amount (wt%) of La in a thorium pyrovanadate sample.

2.1.1. Catalyst characterization

The surface area measurements were carried out on a Quantachrome Autosorb-1 instrument. The samples were dehydrated in vacuum at 250 °C for 4 h prior to an analysis. The physical adsorption and desorption isotherms were recorded at 77 K. The N_2 adsorption BET surface area of ThV_2O_7 was found to be 1.2 $m^2\ g^{-1}$ and that of La substituted sample was around 3.4 $m^2\ g^{-1}$.

The effect of La doping on structural features was investigated using FTIR spectroscopy (JASCO model-60 Spectrophotometer). The samples mixed with KBr powder and pressed into thin pellets were used for this purpose. The powder XRD patterns were taken on a Philips model-PW 1710, diffractometer equipped with a monochromator and Ni-filtered Cu Kα radiation.

2.1.2. Temperature programmed reduction

The TPR patterns were recorded on a Thermoquest TPDRO-1100 analyzer in temperature interval of 27–900 °C (heating rate: 6 °C min^{-1}, gas flow: 20 ml min^{-1}) and in an atmosphere of H_2 (5%) + Ar. The effluents were passed through a soda lime trap prior to analysis by TCD. A 0.021 ± 0.0015 g aliquot of each sample was loaded for a TPR experiment and the sample was subjected to a 2 h pretreatment in helium at 350 °C prior to recording of a TPR run.

2.2. Catalytic activity

A catalyst sample was given a pretreatment for 10 h at 350 °C in N_2 flow of 60 ml min^{-1} prior to activity measurement. The reaction was performed with a feed of methanol in N_2 (0.13:1.0 mole ratio, 60 ml min^{-1}) employing a fixed bed catalytic microreactor unit (from ARB agency, Baroda), operating at atmospheric pressure. A pre-heater assembly in this unit helped in maintaining the reactants at a desired temperature and also ensured a steady flow of reactant stream on the catalyst bed along with the carrier gas. The effluents were passed through a condenser/collector unit for the separation of liquid and gaseous products.

The catalyst sample (0.5 g) was held in between two quartz wool plugs. The products were analyzed on-line using a gas chromatograph (Netel chromatographs) equipped with thermal conductivity and flame ionization detectors connected in tandem. Porapaq-q and molecular sieve columns were employed for product separation. The measurements were continued till about 2 h and by that time a steady state was normally reached.

3. Results

3.1. X-ray diffraction

The powder X-ray diffraction (XRD) patterns of different substituted samples are shown in Fig. 1. The XRD pattern for a sample with x = 0 (Fig. 1a) matched with the standard orthorhombic phase of ThV_2O_7 (JCPDS 24–1330). On substitution of La in place of Th and for value of x in range of 0.2–0.5, the formation of two new phases was observed (Fig. 1b–e). Thus, the set of XRD lines appearing at 2θ values of 18.1°, 24.12°, 32.31°, and 49.4° and marked as * in Fig. 1b

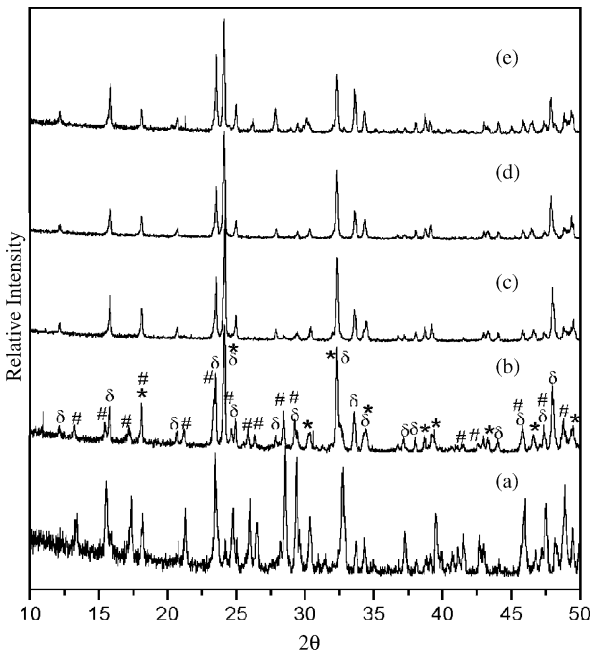

Fig. 1. XRD powder patterns of $La_xTh_{1-x}V_2O_{7-\delta}$ samples with different x values of: (a) 0, (b) 0.2, (c) 0.3, (d) 0.4, and (e) 0.5. Lines marked as #, * and δ represent the ThV_2O_7, $PbLaTh(VO_4)_{3-\delta}$, and $Th(VO_3)_4$ phases, respectively.

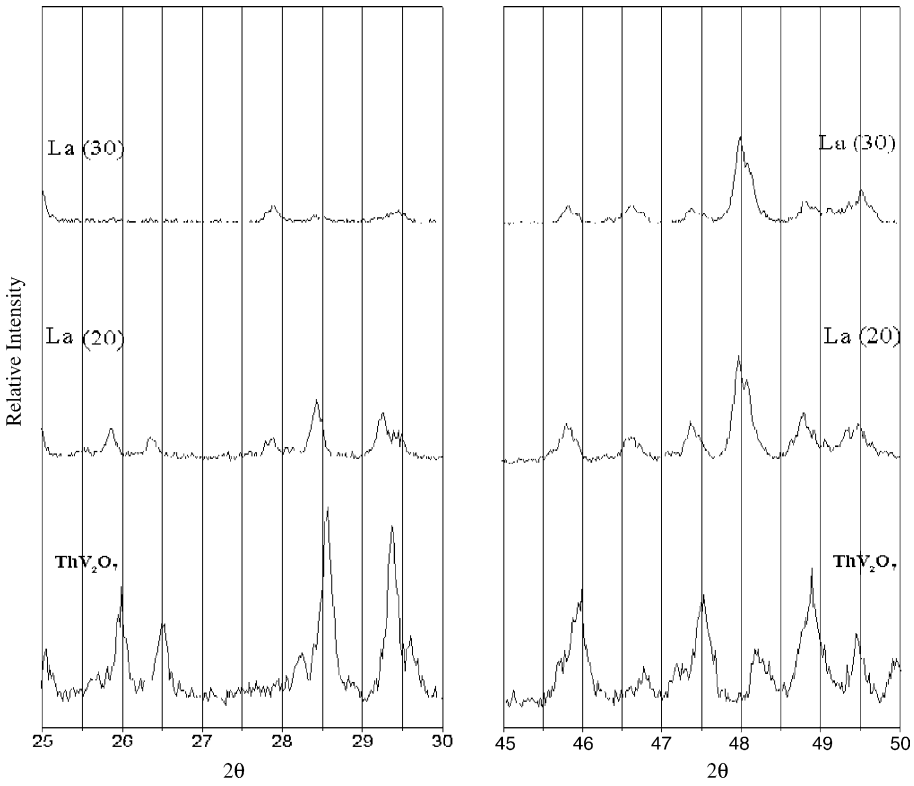

Fig. 2. Segments of XRD powder patterns of ThV_2O_7, La(20) and La(30) samples, highlighting a line shift as a result of La substitution.

are similar to that reported for tetragonal $PbLaTh(VO_4)_3$ phase (JCPDS 36–183) [4]. Another set of lines appearing at 2θ values of 15.8°, 23.4°, 24.1°, 33.6°, 47.9° and marked as δ in this figure match with the XRD profile of $Th(VO_3)_4$ (JCPDS 24–1330). It may also be noticed that the intensity of XRD reflections due to parent thorium pyrovanadate (marked as #) decreased simultaneously and at the same time the position of all the XRD lines of ThV_2O_7 shifted marginally to lower angle. Fig. 2 presents the limited region XRD patterns of ThV_2O_7, La(20), and La(30) samples so as to highlight the influence of substitution on XRD reflections. Data in Figs. 1 and 2 reveal that the content of these three phases, i.e.ThV_2O_7, $LaTh(VO_4)_{3-\delta}$, and $Th(VO_3)_4$, depends upon the value of x in a particular sample. A quantitative evaluation was however found to be difficult because of the fair amount of overlap between the XRD lines corresponding to above mentioned three phases. It is however seen clearly in Fig. 2, that the intensity of 28.56° line, which is exclusively due to parent ThV_2O_7 phase with no overlap, decreases progressively with increase in value of x. Thus, the samples with composition $x \geq 0.4$ comprise mainly of $LaTh(VO_4)_{3-\delta}$ and $Th(VO_3)_4$ phases (Fig. 1d), even though the presence of small amounts of parent phase may not be completely ruled out that may be below the detection limit of XRD technique. At the same time, the prominent XRD lines at 28.56°, 29.38°, 47.51°, and 48.90° get shifted on lanthanum substitution to 28.43°, 29.25°, 47.37°, and 48.79°, respectively, exhibiting a 2θ-shift of ∼0.12° (Fig. 2). These observations may be attributed to the distortion in the ThV_2O_7 lattice because of the substitution of La at A-sites. The possibility of substitution at Th site in $Th(VO_3)_4$ phase is however ruled out since no shift was observed in the XRD lines arising due to this composition (Fig. 1). The various phases identified in La substituted compositions are listed in Table 1.

3.2. IR spectroscopy

The absence of IR band characteristic of V_2O_5 group (∼1020 cm^{-1}) [5] in all the spectra, confirms the completion of the reaction. The existence of multiple phases in La substituted samples, as revealed by XRD results, is supported by IR results also. Thus the FTIR spectrum of ThV_2O_7 (Fig. 3a) exhibits at least two sets of vibrational bands. The IR bands at 973sh, 968, 910, 880, 840, and 818 cm^{-1} are due to VO_3 stretching and the bands at 770 and 690 cm^{-1} may be identified with V–O–V stretching in V_2O_7 unit [6]. On the other hand, the IR spectrum of La(20) (Fig. 3b) comprises of additional bands at 960, 890, 798, 775, 630, and 484 cm^{-1} which may be assigned to symmetric ν_1, asymmetric ν_3 and defor-

Table 1
Identification of phases present in $La_xTh_{1-x}V_2O_{7-\delta}$ using XRD

Sample	x	Phases identified
ThV_2O_7	0.0	ThV_2O_7
La(20)	0.2	$La_xTh_{1-x}V_2O_7$ + $LaTh(VO_4)_{3-\delta}$ + $Th(VO_3)_4$
La(30)	0.3	$La_xTh_{1-x}V_2O_7$ + $LaTh(VO_4)_{3-\delta}$ + $Th(VO_3)_4$
La(40)	0.4	$LaTh(VO_4)_{3-\delta}$ + $Th(VO_3)_4$
La(50)	0.5	$LaTh(VO_4)_{3-\delta}$ + $Th(VO_3)_4$

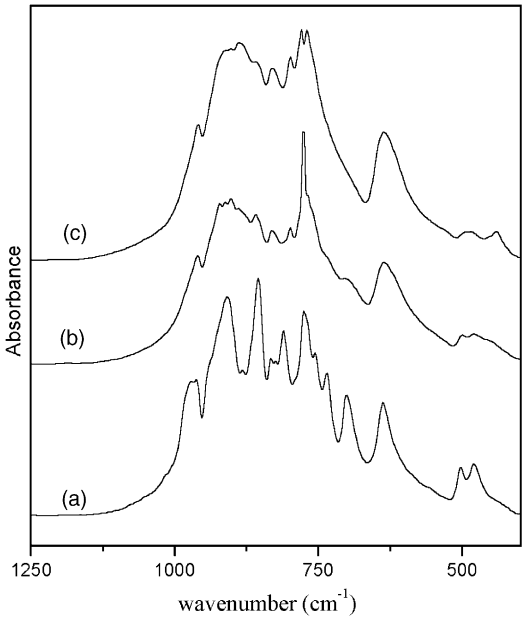

Fig. 3. FTIR spectra of $La_xTh_{1-x}V_2O_{7-\delta}$ samples with different x values: (a) 0, (b) 0.2, and (c) 0.4.

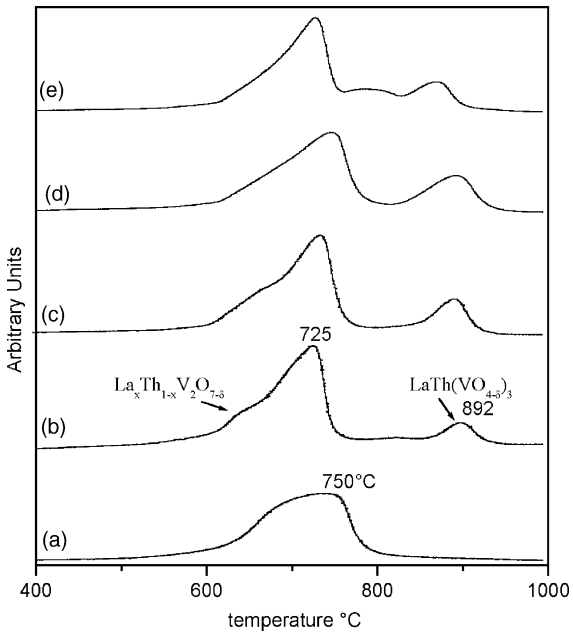

Fig. 4. Comparison of TPR profiles of different $La_xTh_{1-x}V_2O_7$ samples for different values of x: (a) 0, (b) 0.2, (c) 0.3, (d) 0.4 and, (e) 0.5.

mation $\nu_3 + \nu_4$ vibrations of VO_3^{4-} group, indicating the formation of $Th(VO_3)_4$ phase [6]. In addition, bands at 887, 831, and 444 cm^{-1} are also seen in Fig. 3b, which may be assigned to symmetric stretching of VO_2/VO_4 units and in-plane deformation band of VO_2 unit of orthovanadate (VO_4^{3-}) phase [4,6]. It is also observed that the intensity of the IR bands due to pyrovanadate phase decreases with the increasing value of x and at the same time the intensity of a band at ~775 cm^{-1} grows progressively. The 775 cm^{-1} band is characteristic of thorium metavanadates, $Th(VO_3)_4$. These results confirm the progressive transformation of original pyrovanadate phase to metavanadate and orthovanadate phases in case of La(20) and La(40) samples as a result of lanthanum substitution (Fig. 3a–c).

3.3. Temperature programmed reduction

Curves a–e in Fig. 4 present the temperature programmed reduction profiles of La–Th–V oxides of different compositions. It can be seen in TPR profile of ThV_2O_7 (Fig. 4a), that the sample is stable in H_2 up to a temperature of ~500 °C and the subsequent reduction occurs in two stages giving rise to a shoulder band at ~660 °C and the main broad TPR band at ~750 °C. These two TPR bands in Fig. 4a may be attributed to reduction of vanadium at two distinct lattice sites, as is well known [7]. Addition of lanthanum resulted in significant changes in TPR profiles. First, the intensity of 660 °C band increased with the addition of up to ~20% La and decreased again with the further increase in La content. A shift to the lower temperature in this band is also noticeable in the pattern b of Fig. 4. Second, the temperature band of 750 °C shows a shift to lower values with increase in La content and then increases again for the higher values of x. The intensity of this band also changes considerably with the increasing content of La. Another feature noticeable in Fig. 4b, d pertains to development of new TPR bands at around 825 and 900 °C, the intensity of which depended again on the value of x. The hydrogen consumption related to individual TPR band and the variation in temperature maximum (T_m) are shown in Table 2 for a comparative evaluation. The increase in the intensity of 660 °C band in La(20) sample as seen in data of Table 2 and Fig. 4b may be attributed to formation of a

Table 2
Hydrogen consumption corresponding to individual bands in TPR profiles of $La_xTh_{1-x}V_2O_{7-\delta}$ mixed oxides

Sample	First peak		Second peak		Third peak		Total H_2 consumption (μmol/g)
	Temperature (°C)	H_2 consumption (μmol/g)	Temperature (°C)	H_2 consumption (μmol/g)	Temperature (°C)	H_2 consumption (μmol/g)	
ThV_2O_7	660	800	750	2075	–	–	2875
La(20)	630	1284	723	1680	892	504	3486
La(30)	650	1017	733	2119	890	690	3826
La(40)	660	800	746	2879	893	854	3733
La(50)	660	855	727	1854	794–871	1196	3905

nonstoichiometric phase that would be more susceptible to reduction compared to ThV_2O_7. Based on XRD results described above this could be identified with development of new $La_xTh_{1-x}V_2O_{7-\delta}$ phase. The TPR bands in Fig. 4b–d at temperature above 800 °C could similarly be ascribed to formation of other two secondary phases viz. $LaTh(VO_4)_{3-\delta}$ and $Th(VO_3)_4$, the presence of which is confirmed again from XRD results. Another remarkable feature of TPR results was the temperature reproducibility of respective profiles. Thus, while the T_{max} in case of ThV_2O_7 shifted to higher temperature by ∼60 °C during the recording of successive second or third cycles of TPR, in the substituted compositions this shift was restricted to ∼10–15 °C.

3.4. Catalytic activity

Fig. 5 presents the catalytic activity of ThO_2, ThV_2O_7 and La substituted ThV_2O_7, samples for the transformation of methanol in temperature region 150–500 °C. As seen in Fig. 5a, thorium oxide shows very poor catalytic activity with reaction onset temperature of 350 °C and a maximum conversion of ∼12% at a temperature of 425 °C. In the case of thorium pyrovanadate, while the onset temperature was almost the same, a higher conversion of up to 60% was observed, as shown in Fig. 5b. The reaction products were mainly water (∼50%), methane, carbon dioxide and dimethyl ether. In addition, small quantities of methyl formate, formic acid, ethane and dimethoxy methane were also formed. While the yield of water remained almost the same, the amount of other products depended upon reaction temperature. The substitution of thorium by lanthanum up to 20% resulted in significant change in catalytic behavior. For instance, the reaction onset

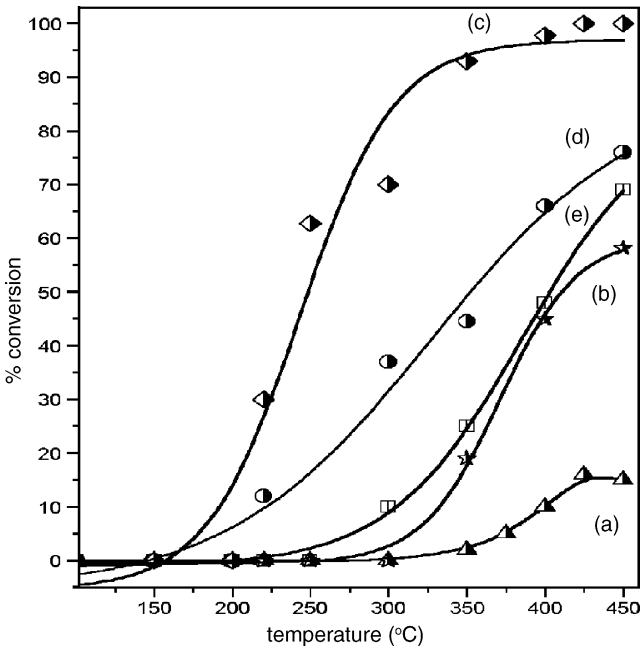

Fig. 5. The catalytic activity of: (a) ThO_2, (b) ThV_2O_7, (c) $La_{0.2}Th_{0.8}V_2O_{7-\delta}$, (d) $La_{0.3}Th_{0.7}V_2O_{7-\delta}$, and (e) $La_{0.5}Th_{0.5}V_2O_{7-\delta}$ catalysts for reaction of methanol at different temperatures.

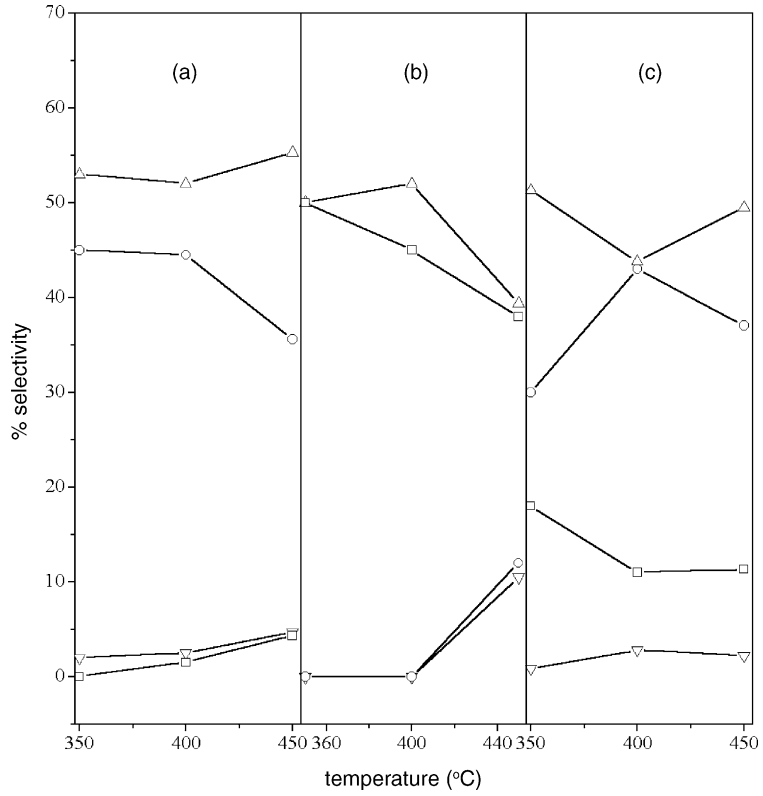

Fig. 6. Temperature dependant product selectivity for reaction of methanol over different samples: (a) ThV_2O_7, (b) $La_{0.2}Th_{0.8}V_2O_{7-\delta}$, and (c) $La_{05}Th_{0.5}V_2O_{7-\delta}$. (–▽–) CO_2, (–◯–) CH_4, (–△–) H_2O, (–□–) DME.

temperature was lowered to 150 °C (Fig. 5c). In addition, almost 100% conversion of methanol was observed at reaction temperatures above 325 °C. The catalyst activity, however, decreased progressively with increasing La content values (Fig. 5d and e). As seen in curves a–e of Fig. 5 the activity of different samples for the reaction of methanol at 400 °C, followed the following trend as a function of the value of *x*

$$La(20) > La(30) > La(50) > ThV_2O_7 > ThO_2$$

Furthermore, the substitution by La improved the catalyst stability and no loss of catalytic activity was detected for all the substituted samples, when the measurements were continued for a period of 3–4 h, under continuous flow of methanol.

The substitution of thorium by La resulted not only in modification of catalytic activity but also in its selectivity. Thus, the La(20) and La(30) samples produced considerably higher amounts of dimethyl ether (DME) while the yields of methane and carbon dioxide decreased. The selectivity data for representative catalyst samples are given in Fig. 6.

3.5. Catalyst stability during the reaction and the successive cycles of reduction/reoxidation

The phase stability of a sample depended upon the La content. Thus La(20) and La(30) samples exhibited a remarkable stability when exposed to methanol at different temperatures up to 450 °C and no changes were observed in the component phases for reaction periods of 8–12 h. For instance, curves a and b in Fig. 7 show XRD patterns of La(30) sample prior to and after catalytic reaction, respectively. On the contrary, the samples with higher lanthanum content were unstable under identical conditions and the typical XRD patterns of La(50), recorded prior to and after the reaction of methanol, are given in curves c and d in Fig. 7. The absence of XRD lines due to $Th(VO_3)_4$ phase present originally in La(50) indicate the transformation of this phase to an oxygen rich $LaTh(VO_4)_{3-\delta}$ phase on reaction with methanol. The high yields of methane during the reaction of methanol over La(50) (Fig. 6c) supports this viewpoint.

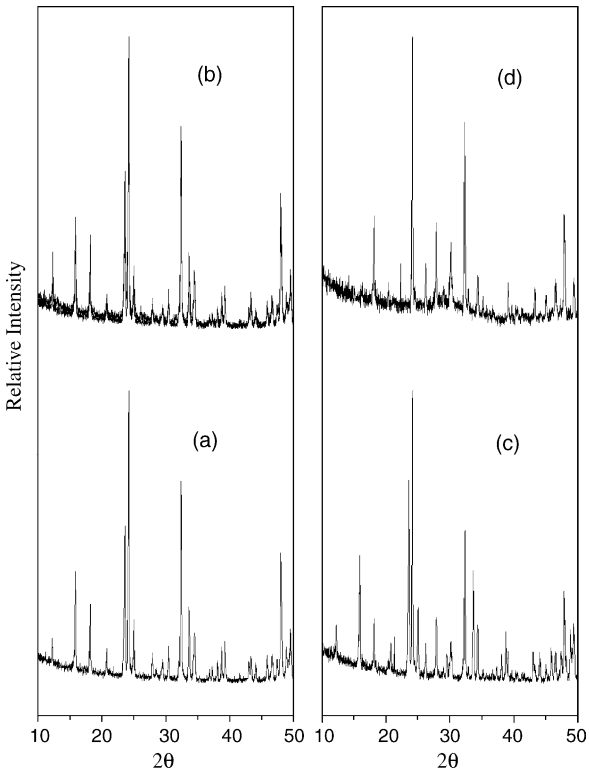

Fig. 7. Comparative XRD patterns of $La_{0.3}Th_{0.7}V_2O_{7-\delta}$ (a, b) and $La_{0.5}Th_{0.5}V_2O_{7-\delta}$ samples (c, d), prior to (a, c) and after (b, d) reaction of methanol.

4. Discussion

La substitution in ThV_2O_7 resulted into a multiphase system and the various phases present were $La_xTh_{1-x}V_2O_{7-\delta}$, $LaTh(VO_4)_{3-\delta}$ and $Th(VO_3)_4$. The relative concentration of these phases in a particular sample depended upon the value of *x*. It is also to be noted that up to La 20% substitution, sample exhibits highest catalyst activity and also a significant lowering of onset temperature for the reaction of methanol at different temperatures in region 150–450 °C. The higher substitutions resulted in the progressive reversal of this trend (curves d and e of Fig. 5). Since the yield of water for reaction at different temperatures is around 50% (Fig. 6) irrespective of the sample composition, the dehydration of methanol may be regarded as the primary step. It is of interest to note here that the enhancement of catalytic activity and also the selectivity for the production of dimethyl ether is not related directly with the presence of new crystallographic phases (i.e., $LaTh(VO_4)_{3-\delta}$ and $Th(VO_3)_4$), since the samples with higher lanthanum content shows poorer activity (Fig. 5d and e) as compared to La(20) sample(Fig. 5c). We may thus argue that the higher activity of La(20) is derived from a pyrovanadate $La_xTh_{1-x}V_2O_{7-\delta}$ phase, where a part of Th lattice sites are occupied by La, and the existence of which is evident from XRD results (Fig. 2). As it is well documented, the structure of ThV_2O_7 is built from $(VO_3)_x$ chains of corner shared VO_4 tetrahedra and independent VO_4 tetrahedra [7]. Thus, the La substitution at Th sites perturbs thorium polyhedra and simultaneously results in the formation of secondary phases, such as $LaTh(VO_4)_{3-\delta}$ and $Th(VO_3)_4$ (Figs. 1 and 3). The TPR results of Fig. 4 reveal that one of these phases in La(20) sample is reducible at a comparatively lower temperature while the other one is responsible to a high temperature peak in TPR profile of Fig. 4c. It is thus likely that the species that reduce at ∼660 °C are basically responsible for enhancement of catalytic activity and may be identified with the $La_xTh_{1-x}V_2O_{7-\delta}$ phase of La(20) samples since the substitution of lower-valent La^{3+} in place of Th^{4+} would lead to increased number of vacant oxygen sites and hence to the greater O^{2-} ion mobility in crystal lattice. These inferences tend to find support in H_2 consumption data for first peak in TPR profile as given in Table 2. On the other hand, other new

phases such as $LaTh(VO_4)_{3-\delta}$ are expected to reduce at a higher temperature and therefore may not play an active role in catalytic dehydration of methanol. The activity trend in La substituted samples as mentioned above confirms that the sample having highest content intensity of $LaTh(VO_4)_{3-\delta}$ phase (i.e. La(50)) is least active catalytically. From data given in Table 2 it is clear that the H_2 consumption of TPR band at >800 °C increases with increase in La substitution, and this value is highest for La(50) sample. As is evident from XRD results in Table 1, even though La(20) and La(30) samples consist of similar crystallographic phases the intensity of XRD line due to nonstoichiometric phase $La_xTh_{1-x}V_2O_{7-\delta}$ decreases considerably in case of La(30) sample. This finds a correlation in decrease of catalytic activity of sample La(30) (Fig. 5d). We may thus infer that the progressive decrease in catalytic activity in Figs. 5d and 5e as compared to that in Fig. 5c is related to growth of a $LaTh(VO_4)_{3-\delta}$ phase. It has similarly been demonstrated in our earlier studies [2,3] that the catalytic activity of thorium metavanadate, $Th(VO_3)_4$ samples decreased progressively on formation of $(VO_4)^{3-}$ ions as a result of manganese substitution at B sites. Our results thus indicate that the catalytic activity of a particular sample may depend upon the ratio of various crystallographic phases mentioned above.

The higher selectivity for the formation of dimethyl ether in case of La(20) samples and for formation of CH_4 in case of La(50) indicated that the course of the reaction in each case is governed by the stoichiometry and the structural characteristics of a sample. The simultaneous formation of water and carbon dioxide suggests again that the participation of lattice oxygen may play an important role in deciding the activity and selectivity of a sample. Similarly, the stability of a sample during methanol reaction depended upon the extent of substitution, the La(20) sample exhibiting the best results. The higher methane selectivity of both ThV_2O_7 and La(50) sample (Fig. 6a and c) are indicative of their oxidation and hence phase transformation during the reaction. On the other hand the crystallographic phase of La(20) is more stable (Fig. 7a and c) and is resistant to further reoxidation. These results indicate the importance of nonstoichiometry in imparting the high activity and stability to a sample even though a quantitative correlation is not possible at this stage between the individual phases generated in a sample as a result of substitution and its catalytic activity or selectivity.

5. Conclusions

ThO_2 is found to be a poor catalyst for methanol decomposition/dehydration reaction as compared to a mixed oxide phase ThV_2O_7. La doping in ThV_2O_7 results in further improvement of catalytic activity and also leads to a better compositional stability. The maximum conversion of methanol is observed at 20% La substitution, resulting in lowering of reduction temperature. In addition to higher catalytic activity, greater selectivity for formation of dimethyl ether was also obtained. The factors responsible for these catalytic and redox properties of substituted ThV_2O_7 samples are identified as generation of nonstoichiometric phase, where involvement of lattice oxygen plays an important role.

References

[1] B.M. Weckhuysen, D.E. Keller, Catal. Today 78 (1–4 SPEC) (2003) 25.
[2] M.R. Pai, B.N. Wani, N.M. Gupta, J. Mater. Sci. Lett. 21 (2002) 1187.
[3] M.R. Pai, B.N. Wani, N.M. Gupta, Prog. Cryst. Growth Charac. 45 (2002) 107.
[4] M.A. Nabar, B.G. Mhatre, J. Solid. State Chem. 45 (1982) 135.
[5] C.T. Au, W.D. Zhang, J. Chem. Soc., Faraday Trans 93 (1997) 1195.
[6] G. Busca, G. Ricchiardi, J. Chem. Soc., Faraday Trans. 90 (8) (1994) 1161.
[7] M. Quarton, A. Rimsky, W. Freundlich, CR Acad. Sci. Paris Ser-c 271 (1970) 1439.